

[ Article ID ] 1003 - 6326(2000)06 - 0749 - 04

## Crystalline structure and morphology of X phase in Cu-Al-Ni-Mn-Ti alloy<sup>①</sup>

WANG Ming-pu(汪明朴), YANG Jie(杨杰), LI Zhou(李周),  
WANG Yan-hui(王艳辉), WANG Zhi-wei(王志伟)(Department of Materials Science and Engineering, Central South University,  
Changsha 410083, P. R. China)

**[ Abstract ]** The composition, morphology, crystalline structure and formation and evolution of X phase in a Cu-12.3Al-2Ni-2Mn-1Ti alloy were studied. The results show that the X phase is a Ti-rich phase with atomic ratio of (Cu + Ni):Ti:Al = 2:1:1 and DO<sub>3</sub> or L2<sub>1</sub> structure; it is directly formed in the liquid phase by crystallization in the process of solidification of the alloy; there forms free particle X phase through the progressive dissolution and breakdown of the interdendritic microstructure in the following homogenization process. The X phase has three different morphologies, i.e. X<sub>L</sub>, X<sub>LS</sub> and X<sub>S</sub>, whose contents in the matrix rely on the heat-treatment conditions.

**[ Key words ]** Cu-Al-Ni-Mn-Ti alloy; X phase; crystalline structure; morphology

**[ CLC number ]** TG146

**[ Document code ]** A

### 1 INTRODUCTION

Copper base shape memory alloys have low costs and good shape memory properties. Their shape memory effects originate from thermoelastic martensitic transformations. A lot of work has been done on the martensitic transformations<sup>[1,2]</sup>, martensitic structures<sup>[3-5]</sup>, ageing effects<sup>[6-8]</sup> and wide hysteresis effects<sup>[9]</sup> and so on. In the recent years, the additions of minor alloying elements into the copper base shape memory alloys, especially the additions of Mn and Ti into the Cu-Al-Ni alloys<sup>[10-14]</sup>, have been drawing great attentions. The additions of elements Mn and Ti will help improve the properties of these alloys, especially there will form a dispersive secondary phase called X phase by adding Ti element. Much work has been done on the X phase in the Cu-Al-Ni-Ti alloys. Adachi et al<sup>[10]</sup> believed that the X<sub>L</sub> is precipitated from the  $\beta$  phase, X<sub>S</sub> is precipitated from the supersaturated matrix on quenching, and X phase is a soft phase. Chang et al<sup>[13]</sup> believed that the X phase is formed by the prior crystallization in the liquid phase at the initial stage of solidification, the X<sub>L</sub> is formed by the spheroidizing of the X phase during the solid solution treatment in the high temperature  $\beta$  phase zone, and the X<sub>S</sub> is precipitated by the nucleation and growth way. But Zhu et al<sup>[14]</sup> believed that the X<sub>L</sub> is produced through the following peritectic reaction:  $L + \beta \rightarrow X_L$ . By taking Cu-12.3Al-2Ni-2Mn-1Ti alloy as an example, the composition, morphology, crystalline structure, and formation and evolution of the X phase were studied in this paper.

### 2 ALLOY PREPARATION AND EXPERIMENTAL METHODS

The nominal composition of the tested alloy is Cu-12.3Al-2Ni-2Mn-1Ti in mass fraction. After medium frequency induction melting in a graphite crucible, the alloy was cast into a slab ingot using a permanent mould. After homogenization treatment at 900 °C for 4 h, the slab ingot was hot rolled into 1 mm thick sheets. Specimens cut along the rolling direction were heat treated at 760 °C for 5 min, 960 °C for 2 h, 960 °C for 2 h then furnace cooled to 760 °C and held for 1 h, and finally cooled on an iron sheet after being taken out from the furnace. Microstructure observations and microhardness measurements were made and composition analysis were realized by X-ray electron probe microanalysis in an X-650 SEM. The TEM observations and phase analyses were made with an H800 TEM.

### 3 RESULTS AND DISCUSSION

#### 3.1 Morphology, composition and crystalline structure

Fig.1 shows the typical bright field images of the tested Cu-Al-Ni-Mn-Ti alloy. It can be seen that the alloy matrix is martensite and the X phase is imbedded in it. The X phase has three different morphologies under the same treatment conditions. The X<sub>L</sub> presents spheric shape with a size of several microns, the X<sub>LS</sub> presents plum blossom like shape with a size of 300 ~ 600 nm (Fig.1(a)), and the X<sub>S</sub> presents cubic or spheric shape with a size of 20 ~ 30 nm

① **[ Foundation item ]** Project (59671024) supported by the National Natural Science Foundation of China

**[ Received date ]** 2000 - 01 - 23 ; **[ Accepted date ]** 2000 - 04 - 10

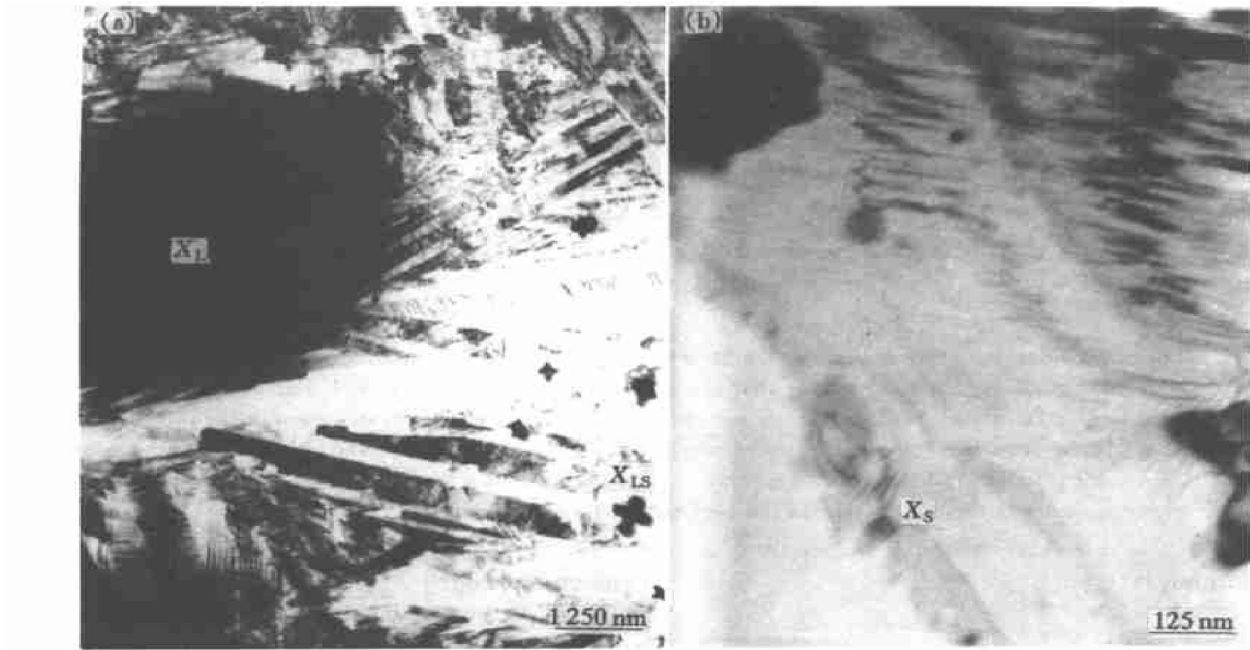


Fig.1 TEM images of Cu-Al-Ni-Ti alloy

( Fig.1( b) ) .

It is found by electron probe microanalysis of the specimens that the matrix martensite is poor in Ti, while the X phase is a Ti-rich phase with the composition of 35.5Cu-26.5Al-23Ti-15Ni in mole fraction which is close to (Cu + Ni): Ti: Al = 2: 1: 1, i.e. the X phase satisfies the chemical formula of (Cu, Ni)<sub>2</sub>TiAl.

Fig.2 shows the electron diffraction patterns of different X<sub>L</sub> particles which can be determined to be the (100)<sup>\*</sup> and (331)<sup>\*</sup> crystal bands of the centered cubic lattice system. The lattice constant is calculated to be 6.06 Å or 5.89 Å respectively by using the two patterns. These values are different from the value of 5.978 Å reported in Ref.[10], which may be caused by the difference of the compositions of X phase in

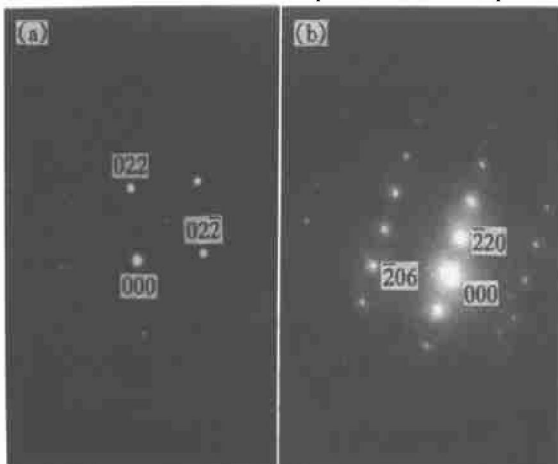


Fig.2 Electron diffraction patterns of X<sub>L</sub>  
( a ) -(100)<sup>\*</sup> ; ( b ) -(331)<sup>\*</sup>

this work and Ref.[10].

It can be deduced from the electronic diffraction patterns that the X<sub>L</sub> possesses DO<sub>3</sub> or L2<sub>1</sub> crystalline structure. The crystalline structure factor of the X<sub>L</sub> can be expressed by

$$F_{HKL} = \{ f_a + f_b \exp[ \pi i( H + K + L) / 2 ] + f_a \exp[ \pi i( H + K + L) ] + f_c \exp[ 3\pi i( H + K + L) / 2 ] \} \cdot \{ 1 + \exp[ \pi i( H + K) ] + \exp[ \pi i( H + L) ] + \exp[ \pi i( K + L) ] \} \quad (1)$$

It can be obtained from expression (1) that:

$$F = \begin{cases} 4(2f_a + f_b + f_c) & H + K + L = 4n \\ 4(2f_a - f_b - f_c) & H + K + L = 4n + 2 \\ 4(f_a - f_c) & H + K + L = \text{odds} \end{cases} \quad (2)$$

These extinction effects agree well with the results of electronic diffractions, thus the previous judgment of the crystalline structure of the X phase is correct.

### 3.2 Formation and evolution of X phase

Fig.3 shows the evolution of microstructure in the homogenization process of the as-cast specimens. There is a large amount of network dendrites in as-cast microstructure and a little precipitation of α phase. It can be seen under high magnification microscope that the interdendritic microstructure is made of irregular deep-colored spheric particles connecting with each other. In the further homogenization process, the dendrites dissolve progressively and separate each other, and form many sphere-like particles dispersively distributed in the matrix. This situation will become stronger with increasing homogenization time. By means of electron probe microanalysis, it is

known that the inter-dendritic microstructure is a Ti-rich phase and with progressing homogenization, the compositions of those free particles separated from the parent phase will more approach to that of the X phase. Therefore it can be concluded that the dendritic microstructure crystallized at the initial stage of solidification is the prototype of the X phase.

Fig. 4 shows the evolution of microstructure of the hot-rolled sheets in the process of heat treatment. The deep-colored particles are the X phase; they are dispersively distributed in the matrix. After heat treatment at 760 °C for 5 min, the distribution of the X phase is more homogeneous, and the content of the  $X_L$  is larger than that of the  $X_{LS}$ . But after heat treatment at 960 °C for 2 h, the previous irregular  $X_L$  spheroidizes progressively, and reduces in content, while the content of the  $X_{LS}$  increases. After 960 °C, 2 h + 760 °C, 1 h treatment, the  $X_L$  becomes irregular in shape again and increases in content, but the content of the  $X_{LS}$  reduces. The above results indicate that the inter-dendritic microstructure in the as-cast alloy is the real resource of the X phase. That is to say, the X phase is formed in the liquid phase by crystallization in the process of solidification. When the temperature is lowered, the melt begins to solidify. Because the solid solubility of Ti in the matrix is small, it is easy to form compounds with the other elements and is considered "impurity" and discharged to the solid-liquid interface front, finally the Ti-rich

phase forms the inter-dendritic microstructure. In the following homogenization process, with the progress of the dissolution of the dendrites, the inter-dendritic microstructure is separated to form free X phase particles, which are dispersively distributed in the matrix and become more homogeneous after hot rolling.

There are several kinds of morphology of the X phase, and the main morphologies are  $X_L$  and  $X_{LS}$ . The finer  $X_S$  is difficult to observe by common optic microscopy. The contents of the  $X_L$  and  $X_{LS}$  depend heavily on the heat treatment conditions. The X phase is formed by the spheroidizing of the original Ti-rich X phase during the solid solution treatment in the high temperature phase zone. At the same time, the  $X_{LS}$  also begins to precipitate by the nucleation and growth way. If the cooling rate is large, then there maybe no enough time for the  $X_{LS}$  to grow up, thus there occurs a large amount of  $X_{LS}$ . If the cooling rate is slow, there is some time for the  $X_{LS}$  to grow up, then there forms the  $X_L$ . But when directly treated at lower temperatures there only takes place the growth of the  $X_{LS}$  and forms the  $X_L$ , thus there also occurs the phenomenon of much  $X_L$  and little  $X_{LS}$ .

### 3.3 Hardness measurement of $X_L$

The hardnesses of the  $X_L$  and the matrix were measured to be Hv 351 and Hv 292, respectively. The  $X_L$  is harder compared with the matrix, which is

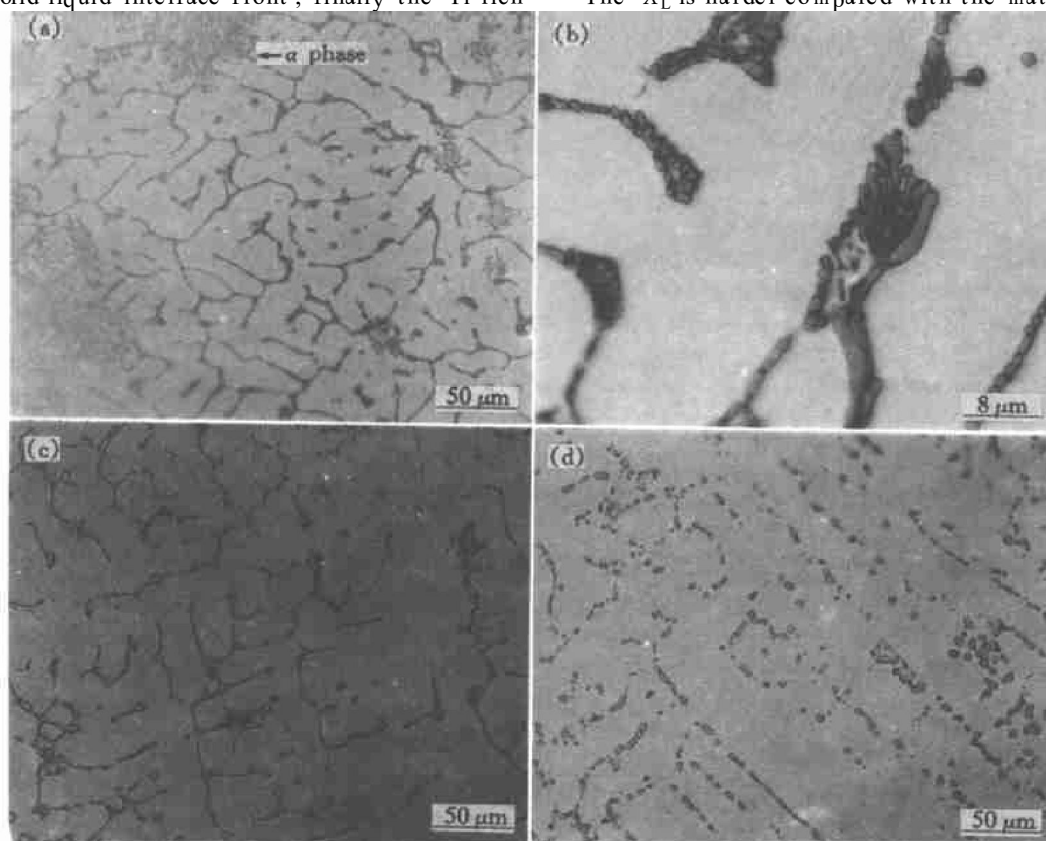
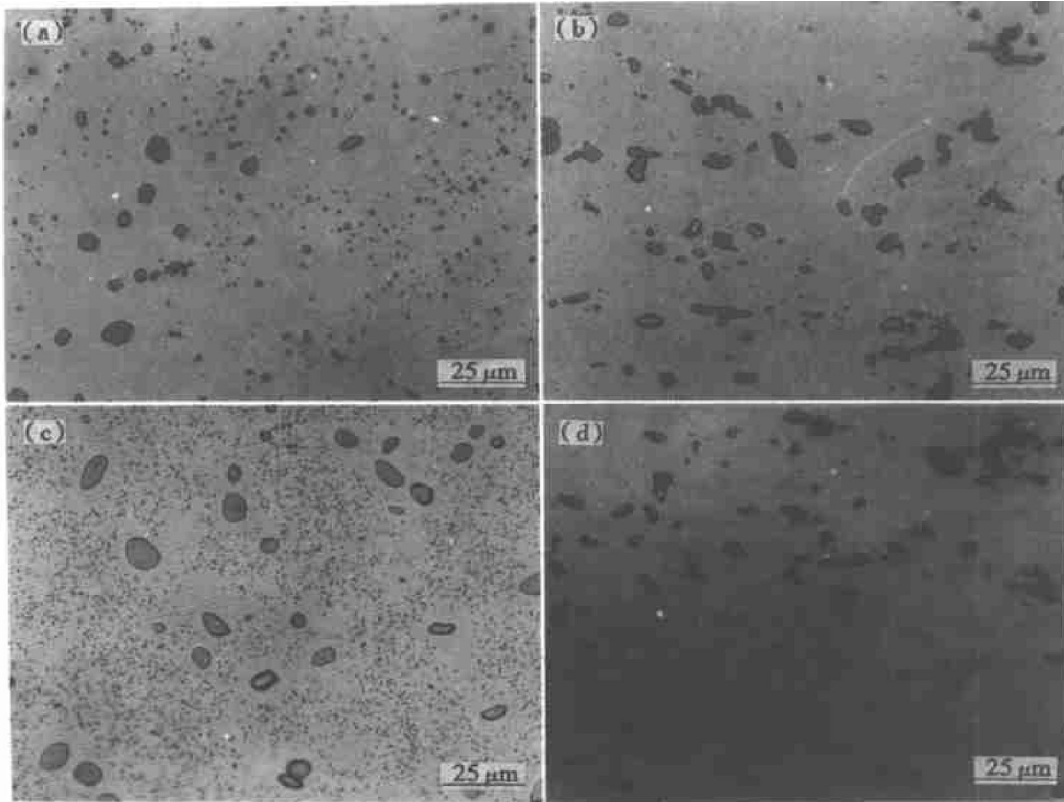


Fig.3 Evolution of microstructure of ingot during homogenization treatment

(a) and (b) — As-cast; (c) —900 °C, 0.5 h; (d) —900 °C, 4 h



**Fig.4** Evolution of microstructure of hot-rolled specimens during heat treatment  
(a) —As-rolled; (b) —760 °C, 5 min; (c) —960 °C, 2 h; (d) —960 °C, 2 h→760 °C, 1 h

different from the result reported in Ref.[10].

#### [ REFERENCES ]

- [1] Shimizu K and Otsuka K. Optical and electron microscope observations of transformation and deformation characteristics in Cu-Al-Ni marman alloys [A]. Perkins J. Shape Memory Effect in Alloys [C]. New York: Plenum Press, 1975. 59 - 87.
- [2] WANG Ming-pu, XIE Xian-jiao, YANG Jie, et al. Metallographic study of thermoelastic martensite transformation in a Cu-Zr-Al alloy. Trans Nonferrous Met Soc China, 1999, 9(4): 741 - 746.
- [3] Suburi T and Wayman C M. The shape memory mechanism in 18R martensitic alloys. Acta Metall, 1980, 28: 15 - 32.
- [4] Adachi K, Perkins J and Wayman C M. Type II twins in self-accommodation martensite plate variants in a Cu-Zr-Al shape memory alloy. Acta Metall, 1986, 34(12): 2471 - 2485.
- [5] WANG Ming-pu, JIN Zhang-peng, YIN Zhi-min, et al. Order state and stability of martensite in an air quenched Cu-Zr-Al alloy. Trans Nonferrous Met Soc China, 1996, 6(3): 113 - 118.
- [6] Tadak T. Aging behaviour of some shape memory alloys and its origin [A]. CHU Y Y. SMM' 94, Proc of the Int Sym on SMM [C]. Beijing: International Academic Publishers, 1994. 31 - 38.
- [7] WANG Ming-pu, JIN Zhang-peng, YIN Zhi-min, et al. Effect of non-isothermal  $\beta$ -phase aging on thermoelastic martensite transformation of Cu-Al-Ni-Mn-Ti alloy [J]. The Chinese Journal of Nonferrous Metals, (in Chinese), 1996, 6(2): 73 - 77.
- [8] CHENG Yan and WANG Ming-pu. Stabilization of martensite in Cu-Zr-Al Alloy and its reverse shape memory effect. Trans Nonferrous Met Soc China, 1998, 8(4): 652 - 656.
- [9] WANG Ming-pu, XU Ge-yin and YIN Zhi-min. Deformation behaviour of Cu-Zr-Al alloys and its effect on transformation hysteresis. Trans Nonferrous Met Soc China, 1995, 5(4): 108 - 113.
- [10] Adachi K, Hamada, Tagawa Y. Gystal structure of X-phase in grain-refined Cu-Al-Ni-Ti shape memory alloys. Scripta Metall, 1987, 21(4): 453 - 458.
- [11] Sure G N and Brown L C. The mechanical properties of grain refined  $\beta$  CuAlNi strain-memory alloys. Metall Trans, 1984, 15A: 1613 - 1621.
- [12] Ratchev P, van Humbeeck J and Delaey L. On the formation of 2H stacking sequence in 18R martensite plates in a precipitate containing Cu-Al-Ni-Ti-Mn alloy. Acta Metall Mater, 1993, 41(8): 2441 - 2449.
- [13] CHANG Feng-lian. Study on the formation of the secondary phase in Cu-Zr-Al-Mn-Ni-Ti alloy. Acta Metall Sinica, (in Chinese), 1995, 31(1): 14 - 18.
- [14] ZHU Wei-hui, WANG Ren-hui, GUI Jia-nian, et al. Fine structure observation of a Cu-Al-Ni-Mn-Ti shape memory alloy [A]. CHU Y Y. SMM' 94, Proc of the Int Sym on SMM [C]. Beijing: International Academic Publishers, 1994. 418 - 422.

(Edited by PENG Chao-qun)